Dynamics of the low-frequency optical phonons of *l*-alanine

Robert A. Crowell and Eric L. Chronister
Department of Chemistry, University of California, Riverside, California 92521
(Received 26 January 1993)

The temperature-dependent (1.1– 100 K) dephasing rates of the two lowest-energy optical phonons of *l*-alanine (42 and 49 cm^{-1}) are obtained from picosecond coherent Raman measurements. The anomalous Raman intensities reported for these modes have been attributed to a thermally induced instability in the 49 cm^{-1} mode, as well as dynamic localization at low temperature [A. Migliori, P. M. Maxton, A. M. Clogston, E. Zirngichi, and M. Lowe, Phys. Rev. B **38**, 13 464 (1988)]. In the present study, thermally induced line broadening is used as a probe of the phonon dynamics, including anharmonic-phonon relaxation.

I. INTRODUCTION

Intermolecular-hydrogen-bonding interactions in molecular crystals can give rise to unique phonon dynamics. The resulting nonlinear phonon interactions can lead to relatively long-lived optical phonons,[1,2] vibrational solitons,[3,4] anomalous Raman intensities,[5] and anomalous thermal conductivities.[6] In addition, intermolecular hydrogen bonding can play a crucial role in determining the molecular crystal structure,[7] and the phonon dynamics can serve as a model for low-frequency dynamics of proteins.[8] In this paper we present temperature-dependent picosecond Raman measurements of the phonon *dynamics* in crystalline *l*-alanine as a means of investigating the proposed instability in the lowest-energy optical phonons.[5]

L-alanine forms large optically clear orthorhombic crystals with four molecules per unit cell[9] in a D_2^4 space group. Due to the low symmetry of the crystal structure, the arrangement of the molecules within the crystal can be viewed as a quasi-one-dimensional chain of hydrogen-bonded molecules. A chain of hydrogen bonds link the molecules along the *c* axis of the crystal, while two other hydrogen bonds bind these chains together in a three dimensional network.

An analysis of the phonon dynamics in *l*-alanine is simplified by the fact that the intramolecular vibrational frequencies are much higher than the frequencies of the external phonon modes, indicating that the external phonon motions are essentially rigid molecule translations and rotations. There are 3 acoustic modes and 21 external optical phonons (4 molecules/unit cell), consisting of 9 translational optical phonons and 12 librons. Polarized single-crystal Raman studies of the lattice modes of *l*-alanine[10–12] have been used to assign the phonon modes and calculate a crystal potential-energy surface in reasonable agreement with the observed phonon frequencies.[11,12] Although the exact phonon eigenvectors are not known, the librons have been visualized in terms of hindered rotations about three perpendicular principle axes *u*, *v*, and *w* defined such that *u* is nearly parallel to the hydrogen-bonded chain (and the crystal *c* axis), *v* is along the long molecular axis, and *w* is perpendicular to the plane of the molecule.[2,13] Although some of the higher-energy B symmetry phonons are difficult to assign,[10] the 42 and 49 cm^{-1} modes have been assigned to *w*-axis librations.[13,2]

The anomalous temperature-dependent Raman intensities of the two lowest-frequency optical phonons in *l*-alanine have been attributed to an instability in the 49 cm^{-1} mode which causes the mode frequency to drop to 42 cm^{-1} when the occupation exceeds seven quanta (≥ 350 cm^{-1}).[5] This instability is also believed to give rise to localization of vibrational energy in the 42 cm^{-1} mode at low temperature.[5,3] The sum of the Raman intensities of the 42 and the 49 cm^{-1} modes has been fit by a Boltzmann population for a single phonon mode, suggesting that these modes may involved the same degree of freedom.[5] However, the Raman intensity study was unable to resolve the narrow Raman linewidths at low temperatures.[5]

The thermal conductivity of a simple dielectric crystal is proportional to the specific heat, the sound velocity, and the phonon scattering time.[14] Although heat conduction in an insulator can be carried largely by the acoustic phonon modes, in *l*-alanine $\frac{3}{4}$ of the heat is believed to be carried by low-energy optical-phonon modes.[15,6] Recent thermal conductivity measurements in crystalline *l*-alanine yielded an exponential decrease with temperature, instead of the expected $1/T$ dependence, from which anharmonic lattice interactions were inferred.[6] If the thermal conductivity of *l*-alanine is in fact reduced by anharmonicity in the lattice forces, then anharmonic-phonon interactions should be reflected in the phonon relaxation and scattering times.

Two previous time-resolved coherent anti-Stokes Raman-scattering (psCARS) studies have been reported for the low-energy Raman-active phonons of *l*-alanine.[1,2] These studies preceded the report of thermal anomalies in the Raman intensities[5] and focused primarily on the correlation of low-temperature phonon linewidths with phonon energy. In the present study, temperature-dependent psCARS measurements are used to obtain the

0163-1829/93/48(1)/172(6)/$06.00

phonon dephasing rates (i.e., linewidths) for the two lowest-frequency optical modes as a probe of the unique anharmonic-phonon interactions in this system.

II. ANHARMONIC-PHONON INTERACTIONS

The optical-phonon mode-Grüneisen parameters are a measure of anharmonic interactions. Furthermore, the instantaneous strain developed by an optical phonon can be used to estimate the magnitude of anharmonic coupling matrix elements.[16] Even without a quantitative measure of the anharmonic interactions, the dependence of the low-temperature phonon relaxation rate on the frequency of the phonon mode can be obtained, assuming that the optically excited phonon decays into counterpropagating Debye acoustic modes.[16] An optically excited phonon mode with negligible crystal moment ($\mathbf{k}\sim 0$) can decay into two acoustic Debye modes through a cubic anharmonic interaction, where conservation of energy and crystal momentum simplifies the low-temperature relaxation process to, $\omega(\mathbf{0})\rightarrow\frac{1}{2}\omega(\mathbf{k})+\frac{1}{2}\omega(-\mathbf{k})$. Low-temperature relaxation measurements of optical phonons in hydrogen-bonded crystals appear to be well described by optical to acoustic relaxation mechanisms.[1,2] The optical-phonon lifetimes T_1 in alanine and in a variety of other amino acid and peptide crystals have been observed to decrease with increasing optical-phonon frequency as $T_1\sim\omega_{\text{opt}}^{-4}$.[1,2]

A. Optical-phonon relaxation

For a lattice of rigid molcules, the crystal potential energy V can be expanded as a power series in terms of molecular displacements (Refs. 17 and 18), $V=\sum_n V_n$, where V_n involves n normal coordinates. Although the harmonic Hamiltonian only involves quadratic terms (i.e., V_2), the potential energy associated with molecular displacements in a real crystal contains cubic and higher-order terms which can lead to an interchange of energy between lattice phonons. Anharmonic theories of lattice dynamics treat the crystal as a system of interacting phonons and cubic phonon interaction terms often dominate the anharmonic Hamiltonian.[17]

Calculations of phonon lifetimes have been performed using the methods of second-order perturbation theory[16,19,20] and temperature Green's functions,[17] and yield the same result if the anharmonic expansion does not exceed cubic and quartic terms. The translational symmetry of a crystal requires that crystal momentum be conserved (i.e., $\mathbf{k}=\mathbf{k}_1+\mathbf{k}_2$ for a cubic process), resulting in a relaxation rate for the phonon $\omega_j(\mathbf{k})$ of branch j and wave vector $\mathbf{k}$,[18,21]:

$$\Gamma_j(\omega)=\frac{18}{\hbar^2}\sum_{\mathbf{k}_1\mathbf{k}_2}\sum_{j_1,j_2}|V(j\mathbf{k},j_1\mathbf{k}_1,j_2\mathbf{k}_2)|^2((\overline{n_{j_1\mathbf{k}_1}}+\overline{n_{j_2\mathbf{k}_2}}+1)\{\delta[\omega-\omega_1(\mathbf{k}_1)-\omega_2(\mathbf{k}_2)]\}$$
$$+(\overline{n_{j_1\mathbf{k}_1}}-\overline{n_{j_2\mathbf{k}_2}})\{\delta[\omega+\omega_1(\mathbf{k}_1)-\omega_2(\mathbf{k}_2)]-\delta[\omega-\omega_1(\mathbf{k}_1)+\omega_2(\mathbf{k}_2)]\}), \tag{1}$$

where the function $V(j\mathbf{k},j_1\mathbf{k}_1,j_2\mathbf{k}_2)$ is related to the cubic anharmonicity V_3 of the lattice intermolecular potential-energy function, and $\overline{n_{j\mathbf{k}}}=\{\exp[\hbar\omega_j(\mathbf{k})/kT]-1\}^{-1}$ is the thermal average occupation number for a phonon from branch j with wave vector $\mathbf{k}$.[18] Each term in the above sum involves a matrix element that couples a mode $\omega_j(\mathbf{k})$ from phonon branch j with a combination of two other modes $\omega_{j_1}(\mathbf{k}_1)+\omega_{j_2}(\mathbf{k}_2)$. An accurate knowledge of the intermolecular potential-energy function is necessary for a quantitative determination of the V coefficients and of phonon relaxation rates in molecular solids.[17]

The magnitude of anharmonic interactions can be qualitatively related to static anharmonic parameters such as the mode-Grüneisen constants. If one assumes a static strain equal to the instantaneous strain of the optical mode, a one-dimensional model yields a relaxation rate which is sensitive to the relative frequency of the optical and acoustic modes at the zone boundary,[16] and predicts a reduced relaxation rate if the optical and acoustic force constants are similar.[16] In a three-dimensional molecular crystal such as *l*-alanine, many of the band-edge librational optical-mode frequencies are *less* than for some of the acoustic modes.

B. Optical-phonon dephasing

In addition to energy relaxation processes, there are exchange and pure dephasing mechanisms which can result in coherence loss without energy relaxation.[21,22] A high-frequency phonon q_j can couple to a low-frequency phonon q_1 through a quartic anharmonic term $V(q_j,q_j,q_1,q_1)$ resulting in a frequency shift to the q_1 mode when the q_j mode is excited. The resulting exchange modulation by the low-frequency phonon can give rise to a temperature-dependent pure dephasing, characterized by a dephasing time T_2' given by[21,22]

$$\frac{1}{\pi T_2'}=\exp\left[\frac{-\hbar\omega_{q_1}}{kT}\right]\frac{(\delta\omega_{q_1})^2T_{q_1}^*}{1+(\delta\omega_{q_1}T_{q_1}^*)^2}, \tag{2}$$

where $T_{q_1}^*$ is the phonon relaxation time of mode q_1, and $\delta\omega_{q_1}$ is the shift in phonon frequency of mode q_1 when mode q_j is vibrationally excited.[21,22] A quartic anharmonic term of the form $V(q_j,q_j,q_1,q_2)$ can also give rise to pure dephasing of the phonon q_j, yielding[23]

$$\frac{1}{\pi T_2'} = \sum_{q_1 q_2} n_{q_1}(n_{q_2}+1)|V(q_j,q_j,q_1,q_2)|^2 \delta(\omega_{q_1}-\omega_{q_2}) \ . \tag{3}$$

If such a mechanism involves a small number of phonon modes of similar energy, the resulting thermally induced line broadening of mode q_j will have the form $\Gamma_{\omega q_j}(T)=\pi V^2 n_2(n_2+1)$ where V is an effective quartic coupling constant.[24] Quartic pure dephasing processes, such as those described by Eqs. (2) and (3), are expected to be most important when cubic phonon processes are forbidden, such as in vibrationally sparse systems.[24] However, since the magnitude of the anharmonic coupling matrix element decreases exponentially with the order of the interaction process (i.e., $|V_3| \gg |V_4|$), cubic processes such as those described by Eq. (1) typically dominate phonon dynamics.

C. Vibrational localization

The effect of vibrational localization on the Raman linewidth is less clear[3,4] than for its effect on the Raman mode intensity.[3–5] Qualitatively, one might expect the lifetime of an optical phonon to be comparable to that of a local phonon mode of the same frequency, since the strain field of a local mode is similar in character to that of an optical mode.[16] However, the theoretical description of the lifetime of a local versus a delocalized phonon[20] is different since relaxation of a delocalized optical phonon[16,20] requires that crystal momentum be conserved. Raman intensity measurements have been used to conclude that the two lowest-energy optical phonons of *l*-alanine involve the same normal coordinates and that a red shift of the 49 cm^{-1} mode occurs when the mode population reaches seven quanta, giving rise the observed 42 cm^{-1} mode.[5] The temperature-dependent phonon dephasing measurements presented in this study are aimed at investigating the proposed dynamic localization of the 42 cm^{-1} mode at low temperature.[5]

A simple model that gives rise to vibrational localization is a linear coupling Hamiltonian, $H=\sum_n (H_\Omega^{(n)}+H_{\omega j}^{(n)}+H_{\rm int}^{(n)})$,[3] where the H_Ω term represents a harmonic mode of frequency Ω on molecule n plus nearest-neighbor dipole-dipole coupling, and the term $H_{\omega j}$ represents a harmonic phonon of frequency ω_j. In the linear coupling model, the modes Ω and ω_j are coupled through $H_{\rm int}=\sum_j \chi_j(a_{nj}+a_{nj}^\dagger)A_n^\dagger A_n$, where $a_n^\dagger, a_n$ and $A_n^\dagger, A_n$ are the creation and annihilation operators for the ω_j and Ω modes, respectively, and where χ_j is the linear coupling constant. This model yields an energy redshift which gives rise to vibrational energy localization, and it predicts a narrower bandwidth for the localized vibration.[3] In such a model, a large linear coupling constant reduces the low-temperature Raman intensity and increases the lifetime of the localized state due to changes in phonon Frank-Condon factors.[3]

The minimum time scale for the self-trapping of vibrational energy is the time required for the mediating phonon to propagate from one molecule to another. When localization is mediated by acoustic phonons this time can be very fast (e.g., $\tau \sim \omega^{-1} \sim 1$ ps), and such a process has been postulated as a significant contributor to the Raman linewidth of the amide-I band in acetanilide.[4] The resulting redshift in the optical-phonon frequency may localize the excitation if its energy drops below the low-amplitude phonon band. Nevertheless, if the trapping time is slower than the lifetime of the optically excited phonon mode, then the Raman linewidth of the higher-energy untrapped mode will be unaffected by the localization process. Since both the 49 and 42 cm^{-1} modes can be optically excited, Raman dephasing measurements provide a probe of the different phonon relaxation mechanisms expected for a delocalized versus a localized phonon.

D. Optical-phonon relaxation in *l*-alanine

The low-temperature relaxation of the lowest-energy optical phonons can occur by fission into two lower-energy acoustic modes. The relatively long optical-phonon lifetimes in hydrogen-bonded molecular crystals at low temperature (versus van der Waals crystals) may be due to the reduced density of acoustic modes resulting from the typically higher Debye frequencies.[25,26,6] In addition, the slight negative *c* axis thermal expansion of *l*-alanine[27] may indicate a coupling between thermally excited molecular librations and translational acoustic modes. Although fission of optically excited librations into two acoustic phonons of one-half the energy is believed to be the relaxation mechanism for the optical phonons in amino acid crystals,[2,3] in more complex hydrogen-bonded crystals, optical to optical phonon relaxation mechanisms are important.[28]

III. EXPERIMENT

L-alanine (Aldrich 99%) was dissolved in deionized water and recrystallized three times. The inhomogeneous contribution to the phonon line shapes decreased upon recrystallization in doubly deionized water; however no further improvement in crystal quality was observed for more than three recrystallizations. *L*-alanine single crystals were grown by slow evaporation (2–3 weeks). Evaporation times of less than one week increased the inhomogeneous contributions to the psCARS decays. Sample crystals were grown to a size of about $5\times5\times2$ mm. The clearest crystals were selected and cleaved to a thickness of about 0.5 mm along either the *bc* or *ac* crystal planes.

The psCARS experiments were performed using a custom-built mode-locked and Q-switched Nd^{+3}:YAG laser (where YAG represents yttrium aluminum garnet) which synchronously pumped two cavity dumped dye lasers. The Q-switch repetition rate was 600 Hz, producing dye laser pulses tunable from 555 to 630 nm with pulse energies of 5–10 μJ, pulse widths of 30–40 ps, and a bandwidth of 1 cm^{-1}. The polarizations of the excitation and probe pulses were aligned using half-wave plates (Oriel) after which they were focused through a 20 cm lens into the sample. The *l*-alanine single crystals were either held in thermal contact with the cold tip of a closed cycle helium refrigerator (Helix CTI-2) for temperatures in the range 9–325 K or immersed in a pumped

liquid helium Dewar for measurements at 1.1 K. Stray light rejection from the pump and probe lasers was enhanced using a high-finesse cutoff filter (Omega 560 EFSP). The CARS signal was dispersed with a 1.5 m monochromator (Spex 1704), detected with a thermoelectrically cooled photomultiplier (Thorn EMI 9635QB) and a lock-in amplifier (Stanford Research Systems SR-510), and digitized and stored (Data Translation DT2821-A/D,IBM/AT-PC). The CARS intensity was measured as a function of probe pulse optical delay using a 1.5 m long stepper motor controlled delay line (Velmex/Unislide) yielding an experimental delay time range of 0–10 ns.

IV. RESULTS AND DISCUSSION

A. Low-temperature Raman lineshapes

Due to the extremely long low-temperature lifetimes of the low-frequency optical phonons of *l*-alanine, it is necessary to characterize inhomogeneous contributions to the psCARS decays due to the inherent imperfections in crystals grown by evaporation, as shown in Fig. 1. Low-temperature (1.1 K) lineshape measurements have been used to obtain the temperature-independent inhomogeneous Gaussian contribution to the line shape, which enables a more accurate determination of the temperature-dependent homogeneous linewidth. Such effects are hard to observe in a frequency domain spontaneous Raman spectrum due to the very narrow linewidths involved. However, characterization and deconvolution of inhomogeneous effects in a psCARS measurement is straightforward due to the relatively long dephasing rate. We found that the optical delay range of ~ 2 ns used in previous experiments[1,2] was insufficient for an accurate determination of the homogeneous and inhomogeneous contributions to the dephasing rate at low

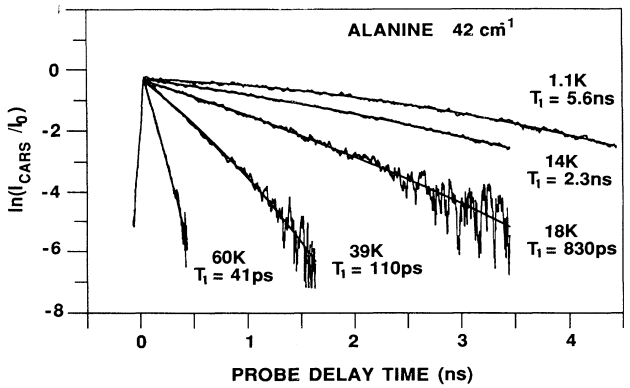

FIG. 1. The decay of the CARS intensity with probe delay is shown for the 42 cm^{-1} optical phonon of *l*-alanine at temperatures of 1.1, 14, 18, 39 and 60 K. The extremely long phonon lifetimes make the dephasing of these phonon modes very sensitive to crystal inhomogeneities. The smooth curves are fits of the data to Eq. (4) using a fixed inhomogeneous linewidth $\Delta\nu_G = 2.4\times10^{-3}$ cm^{-1}, yielding the thermally induced homogeneous linewidth $\Delta\nu_L = (2\pi c T_1)^{-1}$, where T_1 is the phonon lifetime.

TABLE I. The homogeneous ($\Delta\nu_L$) and inhomogeneous ($\Delta\nu_G$) contributions to the phonon linewidths are obtained by fitting the low-temperature ($T=1.1$ K) psCARS results to Eq. (4), as shown in Fig. 1. In addition, an "activation" frequency (ω_c^*) is defined by fitting the temperature-dependent ($T=10$–100 K) homogeneous Raman linewidths to Eq. (5), as shown in Fig. 2.

	$T=1.1$ K		$T=10$–100	
ω_1	$\Delta\nu_G$ 10^{-3} cm^{-1}	$\Delta\nu_L$ 10^{-3} cm^{-1}	ω_c^* cm^{-1}	Γ^* cm^{-1}
42 cm^{-1}	2.4	1.0±0.5	70±3	0.70
49 cm^{-1}	1.8	2.3±0.5		

temperatures. Data acquired with too small a time window appeared exponential even in the presence of inhomogeneous broadening and yielded inaccurate linewidths at low temperature. Therefore, the measurements in this study have been performed using an optical delay time window of 10 ns, enabling deconvolution of inhomogeneous dephasing contributions.

The logarithm of the psCARS intensity decay can be deconvoluted using Eq. (4) to obtain the inhomogeneous and homogeneous contributions to the lineshape,

$$\ln\left[\frac{I_{\mathrm{CARS}}(t)}{I_0}\right] = -(2\pi\Delta\nu_L)t - \frac{\pi c\Delta\nu_G}{\ln 2}t^2 , \qquad (4)$$

where t is the delay time and $\Delta\nu_L$ and $\Delta\nu_G$ are the Lorentzian and Gaussian full width at half maximum contributions to the linewidth in (cm^{-1}), respectively. The resulting low-temperature (1.1 K) psCARS measurements of the homogeneous and inhomogeneous linewidths of the 42 and 49 cm^{-1} modes are listed in Table I. The inhomogeneous contribution to the psCARS decay $\Delta\nu_G$ is determined at low temperature (1.1 K) and once this temperature-independent inhomogeneous contribution is known, Eq. (4) is used to determine the temperature-dependent homogeneous dephasing rate, as shown by the smooth curves in Fig. 1. Although the inhomogeneous contributions to the Raman line shape has been quantified, it still leads to significant uncertainty in the homogeneous linewidth at low temperature. For example, the low-temperature homogeneous linewidths for the 42 and the 49 cm^{-1} modes are $1.0\pm0.5\times10^{-3}$ and $2.3\pm0.5\times10^{-3}$ cm^{-1}, respectively. These extremely small and comparable linewidths suggest similar relaxation processes for these two modes.

B. Temperature-dependent phonon relaxation.

The psCARS decay rates are found to increase with increasing temperature, as shown in Fig. 1. The higher-temperature psCARS decays have also been fit using Eq. (4) with the inhomogeneous contribution $\Delta\nu_G$ fixed from the low-temperature fit. This procedure has been used to obtain the temperature-dependent homogeneous linewidths for both the 42 and the 49 cm^{-1} phonon modes, plotted in Fig. 2. The facile thermal dephasing of these phonons requires that the temperature dependence extend to very low temperatures (1.1 K). This low activation energy can be contrasted with the higher activation

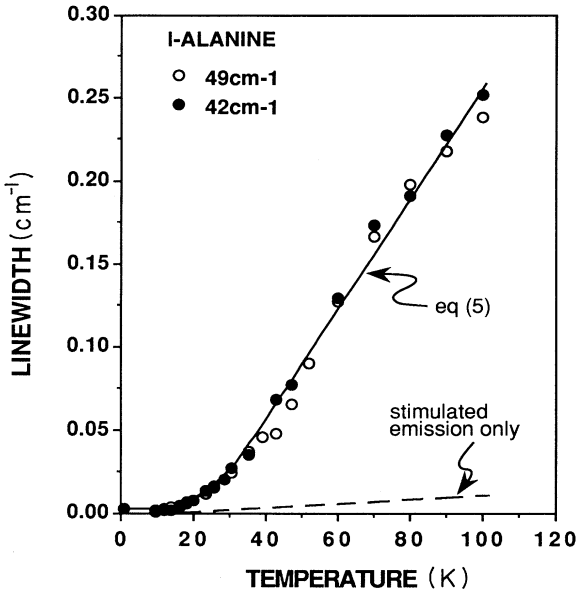

FIG. 2. The homogeneous linewidth of the 42 cm^{-1} (solid circles) and the 49 cm^{-1} (open circles) phonon modes vs temperature. The upper curve is a fit of Eq. (5) to the data, using $\omega_a=\omega_b=23$ cm^{-1}, $\omega_c^*=70$ cm^{-1}, $\omega_d=116$ cm^{-1}, $\Gamma_0=2.2\times10^{-3}$ cm^{-1}, and $\Gamma^*=0.70$ cm^{-1}. The phonon linewidth contribution from stimulated phonon emission is minimal, as indicated by the lower dashed curve.

energies for the thermal dephasing of intramolecular vibrons (typically temperature independent below 30 K).

In the absence of higher-energy optical-phonon modes, stimulated emission of acoustic phonons would be the only thermally induced relaxation process. However, in complex molecular solids, relaxation due to phonon absorption (up conversion) processes contribute to the phonon dynamics and can dominate at higher temperatures. Thus, the phonon linewidth can be expressed as a sum of spontaneous emission, stimulated emission, and phonon absorption (up conversion) processes,

$$\Gamma(\omega_j)=\Gamma_0+\Gamma_0(\bar{n}_a+\bar{n}_b)+\Gamma^*(\bar{n}_c-\bar{n}_d)\ , \tag{5}$$

where $\Gamma(\omega_j)$ is the linewidth of the optically excited state, Γ_0 is the low-temperature linewidth (due to spontaneous relaxation to lower-energy acoustic modes), $\Gamma_0(\bar{n}_a+\bar{n}_b)$ characterizes stimulated phonon emission by decay into a pair of lower-energy phonons $\omega_j\rightarrow\omega_a+\omega_b$, and Γ^* is the coefficient responsible for absorption of a thermally populated phonon, $\omega_c^*+\omega_j\rightarrow\omega_d$. For discussion purposes, Eq. (5) characterizes the summation over cubic decay pathways given in Eq. (1) by "effective" phonon relaxation pathways. If conservation of energy and crystal momentum requirements restrict the possible relaxation channels, and if the energies of the phonons involved are not too different for different relaxation channels, then Eq. (5) can be expected to model the thermal broadening of the phonon linewidth.

The temperature-dependent homogeneous linewidth (obtained from psCARS measurements) for the 42 cm^{-1} (solid circles) and 49 cm^{-1} (open circles) modes, are shown in Fig. 2. Also shown is a fit of Eq. (5) to the data using the parameters $\omega_a=\omega_b=23$ cm^{-1}, $\omega_c^*=70$ cm^{-1}, $\omega_d=116$ cm^{-1}, $\Gamma_0=2.2\times10^{-3}$ cm^{-1}, and $\Gamma^*=0.70$ cm^{-1}. The low-temperature phonon lifetime determines the coupling coefficient for fission of the optical phonon into two acoustic modes Γ_0, while conservation of energy and crystal momentum fixes all the other parameters except ω_c^* and Γ^* (the only parameters adjusted in the fit). The linewidth contribution due to stimulated phonon emission is found to be minimal, as shown by the lower curve in Fig. 2, since Γ^* is over two orders of magnitude larger than Γ_0. Therefore, the thermal broadening of the linewidth is largely due to the absorption of a thermally populated lower-energy mode(s) ω_c^* (i.e., up-conversion due to a process $\omega_j+\omega_c^*\rightarrow\omega_d$).

TABLE II. Band-center frequencies (13 of 21 possible) of the optical phonons of *l*-alanine at 130 K (from Ref. 10).

cm^{-1}
41
49
76
88
96
103
105
108
119
137
145
150
167

The psCARS data are most easily described in terms of a cubic phonon up conversion of the 42 and 49 cm^{-1} modes to higher-energy optical phonons. For example, the activation energy, $\omega_c^*=70$ cm^{-1}, is consistent with a cubic up-conversion process (e.g., 42 $cm^{-1}+70$ $cm^{-1}\rightarrow112$ cm^{-1}). The large number of optical-phonon modes (21, some of which are listed in Table II), and the dispersion in the mode energies with wave vector, virtually guarantees that the cubic process can conserve energy and crystal momentum. For simplicity, the phonon dynamics have been analyzed in terms of effective relaxation pathways, however, the quality of the fit in Fig. 2 was not significantly improved when additional relaxation pathways were included in Eq. (5). Our results are consistent with a previous study which proposed that the 49 cm^{-1} phonon decayed by the absorption of 80 cm^{-1} phonons at temperatures above 25 K.[2] However, the dynamics of the 49 cm^{-1} phonon below 25 K has previously been attributed to the absorption of 40 cm^{-1} phonons.[2] Our lower-temperature data does not indicate a contribution from such a relaxation mechanism, possibly due to a better determination of the homogeneous dephasing rate at lower temperatures.

V. CONCLUSIONS

Raman dephasing measurements have been used as a sensitive probe of thermally induced phonon relaxation

processes for the low-frequency optical phonons of *l*-alanine. Although the temperature-dependent Raman intensity of the 42 cm^{-1} phonon has previously been attributed to dynamic localization at low temperature, our results do not provide additional evidence for such a process. Since crystal momentum does not have to be conserved for the relaxation of a localized phonon, different relaxation pathways should exist relative to a delocalized phonon of similar energy,[20] and thermally induced relaxation processes should be sensitive to these differences. However, we observed similar temperature-dependent Raman dephasing rates for the 49 and 42 cm^{-1} phonon modes, suggesting similar relaxation mechanisms. The results of this study are most readily explained by up conversation to higher-energy optical phonons by the absorption of thermally populated phonons.

[1]T. J. Kosic, R. E. Cline, Jr., and D. D. Dlott, Chem. Phys. Lett. **103**, 109 (1983).
[2]T. J. Kosic, R. E. Cline, Jr., and D. D. Dlott, J. Chem. Phys. **81**, 4932 (1984).
[3]A. C. Scott, I. J. Bigio, and C. T. Johnson, Phys. Rev. B **39**, 12 883 (1989).
[4]G. Careri, U. Buintempo, F. Galluzzi, A. C. Scott, E. Gratton, and E. Shyamsunder, Phys. Rev. B **30**, 4689 (1984).
[5]A. Migliori, P. M. Maxton, A. M. Clogston, E. Zirngichi, and M. Lowe, Phys. Rev. B **38**, 13 464 (1988).
[6]R. S. Kwok, P. Maxton, and A. Migliori, Solid State Commun. **74**, 1193 (1990).
[7]M. C. Etter, J. Phys. Chem. **95**, 4601 (1991).
[8]D. D. Dlott, Annu. Rev. Phys. Chem. **37**, 157 (1986).
[9]M. S. Lehmann, T. F. Koetzle, and W. C. Hamilton, J. Am. Chem. Soc. **94**, 2657 (1972).
[10]Wang and Storms, J. Chem. Phys. **55**, 5110 (1971).
[11]K. Machida, A. Kagayama, and Y. Saito, J. Raman Spectrosc. **7**, 188 (1978).
[12]K. Machida, A. Kagayama, Y. Saito, and T. Uno, Spectrochim. Acta. **34A**, 909 (1978).
[13]E. Loh, J. Chem. Phys. **63**, 3192 (1975).
[14]R. Peierls, Ann. Phys. (Leipzig) **3**, 1055 (1929).
[15]G. A. Slack, Solid State Phys. **34**, 1 (1979).
[16]P. G. Klemens, Phys. Rev. **148**, 845 (1966).
[17]S. Califano, V. Schettino, and N. Neto, *Lattice Dynamics of Molecular Crystals* (Springer-Verlag, Berlin, 1981).
[18]R. G. Della Valle, P. Fracassi, R. Righini, and S. Califano, Chem. Phys. **74**, 179 (1983).
[19]P. G. Klemens, in *Solid State Physics: Advances in Research and Applications,* edited by F. Seitz and D. Turnbull (Academic, New York, 1958).
[20]P. G. Klemens, Phys. Rev. **122**, 443 (1961).
[21]J. Bellows and P. Prasad, J. Chem. Phys. **70**, 1864 (1979).
[22]C. B. Harris, R. M. Shelby, and P. A. Cornelius, Phys. Rev. Lett. **38**, 1415 (1977).
[23]R. M. Hochstrasser and P. N. Prasad, in *Excited States,* edited by E. C. Lim (Academic, New York, 1974), Vol. 1, p. 79.
[24]L. Angeloni, R. Righini, P. R. Salvi, and V. Schettino, Chem. Phys. Lett. **154**, 432 (1989).
[25]A. I. Kitaigorodsky, *Molecular Crystals and Molecules* (Academic, New York, 1973).
[26]M. Daurel, P. Delhaes, and E. Dupart, Biopolymers **14**, 801 (1975).
[27]S. Forss, J. Raman Spectros. **12**, 266 (1982).
[28]E. L. Chronister and D. D. Dlott, Proc. SPIE, **620**, 97 (1986).